The Plant Cell, Vol. 23: 499–514, February 2011, www.plantcell.org

The J-Domain Protein J3 Mediates the Integration of Flowering Signals in *Arabidopsis* [W]

Lisha Shen, Yin Ga Germain Kang, Lu Liu, and Hao Yu[1]

Department of Biological Sciences and Temasek Life Sciences Laboratory, National University of Singapore, 117543, Singapore

The timing of the switch from vegetative to reproductive development in *Arabidopsis thaliana* is controlled by an intricate network of flowering pathways, which converge on the transcriptional regulation of two floral pathway integrators, *FLOWERING LOCUS T* (*FT*) and *SUPPRESSOR OF OVEREXPRESSION OF CONSTANS1* (*SOC1*). *SHORT VEGETATIVE PHASE* (*SVP*) acts as a key flowering regulator that represses the expression of *FT* and *SOC1*. Here, we report the identification of another potent flowering promoter, *Arabidopsis* DNAJ HOMOLOG 3 (J3), which mediates the integration of flowering signals through its interaction with SVP. *J3* encodes a type I J-domain protein and is ubiquitously expressed in various plant tissues. *J3* expression is regulated by multiple flowering pathways. Loss of function of *J3* results in a significant late-flowering phenotype, which is partly due to decreased expression of *SOC1* and *FT*. We further show that J3 interacts directly with SVP in the nucleus and prevents in vivo SVP binding to *SOC1* and *FT* regulatory sequences. Our results suggest a flowering mechanism by which J3 integrates flowering signals from several genetic pathways and acts as a transcriptional regulator to upregulate *SOC1* and *FT* through directly attenuating SVP binding to their regulatory sequences during the floral transition.

INTRODUCTION

The transition from vegetative to reproductive development, known as the floral transition, is tightly controlled by a complex network of genetic pathways in response to various developmental and environmental signals in *Arabidopsis thaliana* (Mouradov et al., 2002; Simpson and Dean, 2002; Blázquez et al., 2003; Boss et al., 2004). The photoperiod pathway monitors seasonal changes in daylength, while the vernalization pathway senses the prolonged exposure to low temperature. The gibberellin (GA) pathway plays a particular promotive role in flowering under noninductive photoperiods, while the autonomous pathway mediates flowering by perceiving plant developmental status. In addition, the thermosensory pathway affects flowering through mediating plant response to ambient temperature signaling. The flowering signals from these multiple genetic pathways ultimately converge on the regulation of two major floral pathway integrators, *FLOWERING LOCUS T* (*FT*) and *SUPPRESOR OF OVEREXPRESSION OF CONSTANS1* (*SOC1*), which in turn activate floral meristem identity genes, mainly *APETALA1* (*AP1*) and *LEAFY* (*LFY*), to initiate the generation of floral meristems (Kardailsky et al., 1999; Kobayashi et al., 1999; Blázquez and Weigel, 2000; Lee et al., 2000; Samach et al., 2000; Liu et al., 2009a, 2009b; Wang et al., 2010).

The integration of flowering signals is regulated by a key repressor complex that consists of two MADS box transcription factors, FLOWERING LOCUS C (FLC) and SHORT VEGETATIVE PHASE (SVP) (Michaels and Amasino, 1999; Hartmann et al., 2000; Li et al., 2008). *SVP* expression is regulated by the flowering signals perceived by the thermosensory, autonomous, and GA pathways (Lee et al., 2007; Li et al., 2008), while *FLC* expression is controlled by the signals from the vernalization and autonomous pathways (Michaels and Amasino, 1999; Sheldon et al., 1999). During the vegetative phase, the interaction of these two potent repressors suppresses *SOC1* expression in whole seedlings and *FT* expression in leaves (Helliwell et al., 2006; Searle et al., 2006; Lee et al., 2007; Li et al., 2008). During the floral transition, stimulatory flowering signals from various flowering pathways except for the photoperiod pathway downregulate the expression of *FLC* and *SVP*, which, in turn, derepresses the expression of *FT* and *SOC1* to allow the transformation of vegetative shoot apical meristems into inflorescence meristems. Although considerable efforts so far have been made to elucidate the flowering regulatory hierarchy involving *FLC* and *SVP*, the underlying mechanism mediating their role in transcriptional regulation of target genes is largely unknown.

In *Arabidopsis*, there is a large and diverse family of molecular chaperones, called J-domain proteins (Miernyk, 2001; Rajan and D'Silva, 2009). Based on the secondary structural assignments for J-domain, which is characterized by four α-helices and an invariable tripeptide of His, Pro, and Asp (HPD motif) after the second helix, a total of 120 J-domain proteins have been identified in *Arabidopsis* and are classified into four types (I, II, III, and IV) (Rajan and D'Silva, 2009). Type I J-domain proteins have a modular sequence containing a J-domain, a Gly/Phe-rich domain (G/F), a CXXCXGXG zinc finger domain, and a less conserved C-terminal domain, whereas the other types of J-domain proteins lack one or more of these domains. The sequential domain organization in type I J-domain proteins is similar to the

[1] Address correspondence to dbsyuhao@nus.edu.sg.
The author responsible for distribution of materials integral to the findings presented in this article in accordance with the policy described in the Instructions for Authors (www.plantcell.org) is: Hao Yu (dbsyuhao@nus.edu.sg).
[W] Online version contains Web-only data.
www.plantcell.org/cgi/doi/10.1105/tpc.111.083048

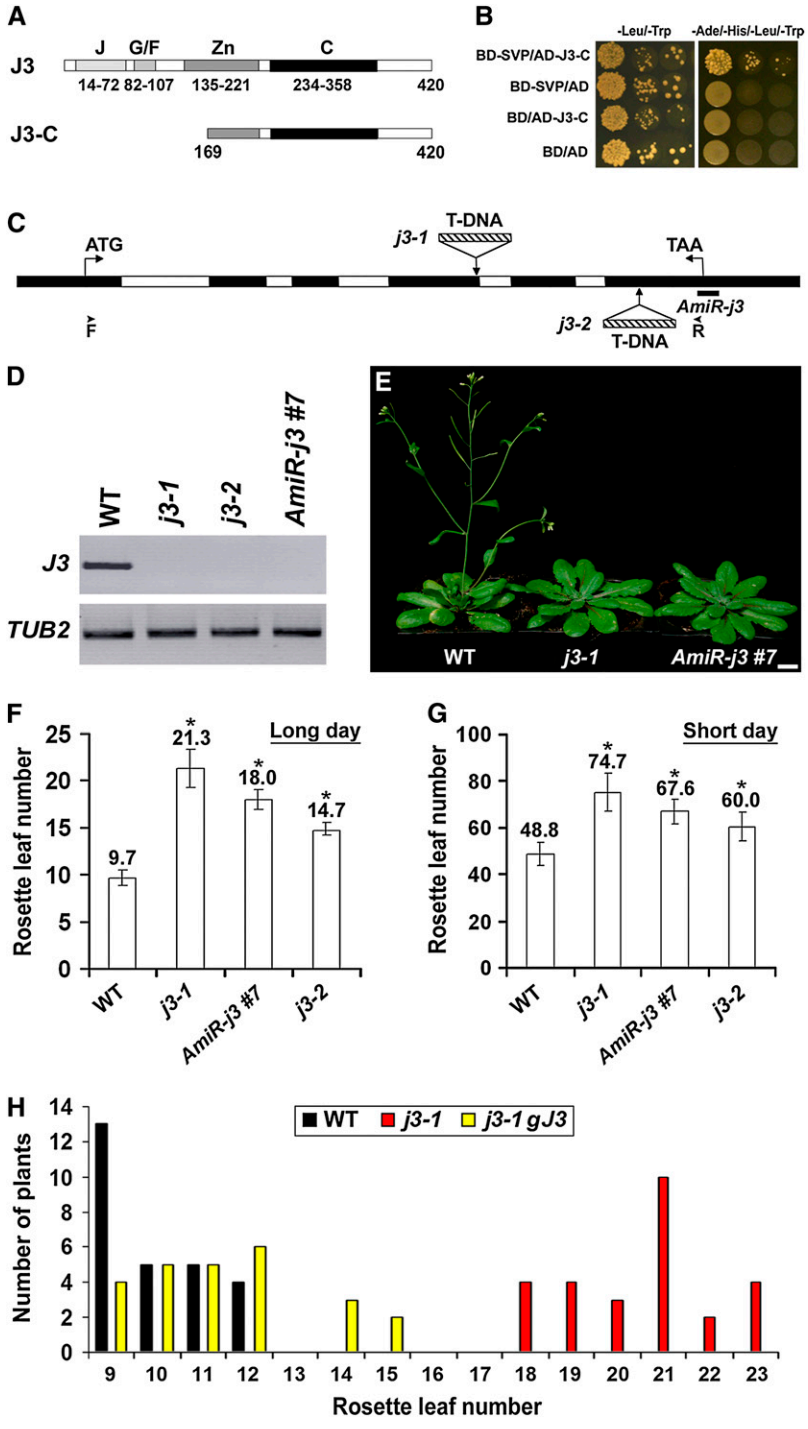

Figure 1. *J3* Regulates Flowering Time in *Arabidopsis*.

(A) Schematic diagram shows the domain structure of J3 whose C terminus (J3-C) was identified from yeast two-hybrid screening using SVP as a bait. J3 contains a J-domain (J) in the N terminus, a G/F-rich domain (G/F), a CXXCXGXG zinc finger domain (Zn), and a C-terminal domain (C).
(B) A yeast two-hybrid assay shows the interaction between J3-C and SVP. Serial dilutions (1:1, 1:10, and 1:50) of transformed yeast cells were grown on SD/-Ade/-His/-Leu/-Trp medium (right panel) and SD/-Leu/-Trp medium (left panel). The C-terminal region of J3 and full-length coding region of SVP were fused to the GAL4 activation domain (AD) in pGADT7 (AD-J3-C) and the GAL4 DNA binding domain (BD) in pGBKT7 (BD-SVP), respectively. The pGADT7 (AD) and pGBKT7 (BD) were used as controls.
(C) Schematic diagram shows the T-DNA insertion sites in *j3-1* (Salk_132923) and *j3-2* (Salk_141625) as well as the target site of the AmiR in *AmiR-j3*.

modular structure of DnaJ/Hsp40 that was originally identified as a 41-kD heat shock protein from *Escherichia coli* (Georgopoulos et al., 1980).

Previous studies have shown that DnaJ interacts with Hsp70, DnaK, and the nucleotide exchange factor, GrpE, to constitute a molecular chaperone complex that functions in many cellular processes (Liberek et al., 1991; Georgopoulos, 1992; Scidmore et al., 1993; Cyr et al., 1994; Bukau and Horwich, 1998; Goffin and Georgopoulos, 1998). Apart from the chaperone activity, DnaJ also functions as a protein disulfide isomerase to catalyze the formation, reduction, or isomerization of disulfide bonds (de Crouy-Chanel et al., 1995; Wang and Tsou, 1998). Furthermore, it has been suggested that DnaJ function is conserved throughout evolution (Caplan et al., 1993; Silver and Way, 1993; Qiu et al., 2006).

In plants, J-domain proteins have been reported to localize in different subcellular compartments and participate in various biological processes (Miernyk, 2001; Rajan and D'Silva, 2009). However, as molecular chaperones are traditionally considered as important components involved in cellular homeostasis under stress conditions, previous studies on plant J-domain proteins have been mainly focused on their functions in plant stress signaling pathways (Wang et al., 2004; Ham et al., 2006; Yang et al., 2010). While there are a few studies reporting the involvement of plant J-domain proteins in developmental processes (Tamura et al., 2007; Kneissl et al., 2009), the molecular basis for their biological functions in plant growth and development is still enigmatic.

In this study, we report that *Arabidopsis DNAJ HOMOLOG 3* (*J3*), which encodes a type I J-domain protein (Zhou and Miernyk, 1999; Rajan and D'Silva, 2009), plays an essential role as a transcriptional regulator in mediating the integration of flowering signals. Loss of function of *J3* significantly delays flowering, which partly results from reduced expression of *SOC1* and *FT*. J3 interacts with SVP in the nucleus and attenuates the capacity of SVP binding to the regulatory sequences of *SOC1* and *FT*. Our results suggest that *J3* perceives flowering signals from several genetic pathways and promotes flowering through directly antagonizing SVP activity in repressing the transcription of *SOC1* and *FT* during the floral transition.

RESULTS

Loss of Function of *J3* Delays Flowering Time in *Arabidopsis*

To elucidate *SVP* function in *Arabidopsis* reproductive development, we previously performed yeast two-hybrid screening to identify its interacting partners (Liu et al., 2009b). Five out of over 50 interactors included the C-terminal part of J3 protein, which contains the 252 amino acid residues from 169 to 420 (Figure 1A). We cloned this C-terminal fragment and confirmed its interaction with SVP by yeast two-hybrid assay (Figure 1B). *J3* encodes a DnaJ-like heat shock protein, which contains a typical modular sequence of type I J-domain proteins (Figure 1A) (Zhou and Miernyk, 1999; Rajan and D'Silva, 2009; Yang et al., 2010). A sequence comparison revealed that J3 homologs shared high sequence similarity across plant species and other eukaryotic organisms, such as yeast (*Saccharomyces cerevisiae*), zebra fish (*Danio rerio*), mouse (*Mus musculus*), and human (*Homo sapiens*) (see Supplemental Figure 1 online).

To investigate the biological function of *J3*, we isolated two T-DNA insertional mutants, *j3-1* and *j3-2*, from The Arabidopsis Information Resource (TAIR; http://www.Arabidopsis.org). *j3-1* and *j3-2* contained a T-DNA insertion in the fourth and last exons, respectively (Figure 1C). There was no detectable full-length *J3* transcript in either homozygous mutant line (Figure 1D). Partial *J3* transcripts upstream of the T-DNA insertion sites were significantly downregulated, while no transcripts could be detected spanning or downstream of the T-DNA insertion sites in *j3-1* and *j3-2* (see Supplemental Figure 2A online). Under long days (LDs) and short days (SDs), both *j3-1* and *j3-2* showed late flowering, while the former possessed a stronger phenotype (Figures 1E to 1G). The F1 progenies from the cross between *j3-1* and *j3-2* flowered later than wild-type plants with an intermediate flowering phenotype compared with the single mutants (see Supplemental Figure 2B online), further indicating that *j3-1* and *j3-2* are allelic. Since *j3-1* was likely a strong mutant allele, we used it for further analyses. To test whether the late-flowering phenotype of *j3-1* can be attributed to the loss of *J3* function, we transformed *j3-1* with a genomic construct (*gJ3*) harboring a 4.5-kb *J3* genomic region that includes 2.2 kb of upstream sequence, the 1.9-kb full coding sequence plus introns, and 0.4 kb of the 3′ untranslated region. Most *j3-1 gJ3* T1 transformants exhibited comparable flowering time to wild-type plants (Figure 1H), demonstrating that *J3* is responsible for the late-flowering phenotype observed in *j3-1*.

To confirm *J3* function in the regulation of flowering time, we also created *J3* knockdown transgenic plants by artificial microRNA (AmiR) interference (Schwab et al., 2006). We generated 25 *AmiR-j3* independent lines that expressed an AmiR specifically targeting at the 3′ region of the *J3* mRNA (Figure 1C), among which 19 lines exhibited different levels of late flowering under LDs. We measured *J3* expression in five selected late-flowering lines and found that the degrees of late flowering in *AmiR-j3*

Figure 1. (continued).

Exons and introns in the coding region are indicated by black and white boxes, respectively. The start codon (ATG) and stop codon (TAA) are labeled. Arrowheads indicate the position of primers used for amplifying full-length *J3* transcript as shown in **(D)**.

(D) RT-PCR shows that the full-length *J3* transcript is undetectable in *j3-1*, *j3-2*, and *AmiR-j3 #7*. *TUB2* was amplified as an internal control. WT, wild type.

(E) *j3-1* and *AmiR-j3* exhibit late flowering under long days. Bar = 1 cm.

(F) and **(G)** Flowering time of *j3* mutants and *AmiR-j3 #7* transgenic plants under LDs **(F)** and SDs **(G)**. Values were scored from at least 15 plants of each genotype. Mean values of rosette leaf number are indicated on top of bars. Error bars denote SD. Asterisks indicate significant difference in flowering time of *j3-1*, *AmiR-j3 #7*, and *j3-2* compared with that of wild-type plants (Student's *t* test, $P < 0.05$).

(H) Distribution of flowering time in T1 transgenic plants harboring the *J3* genomic fragment in *j3-1* background.

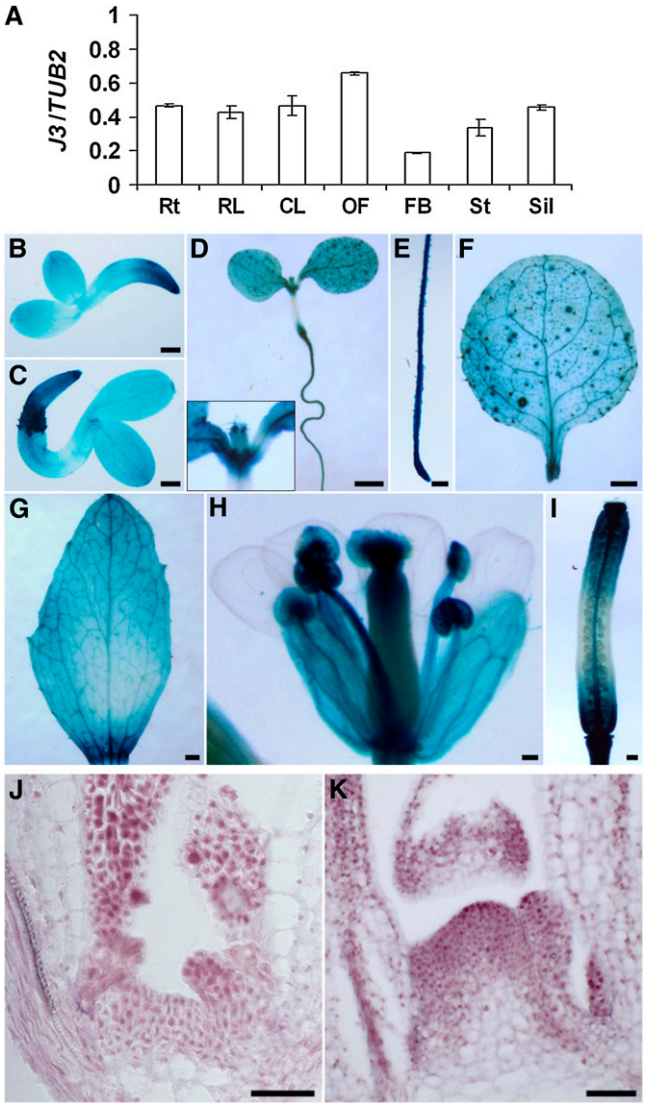

Figure 2. *J3* Is Ubiquitously Expressed in *Arabidopsis*.

(A) Quantitative real-time PCR analysis of *J3* expression in various tissues of wild-type Col plants. Results were normalized against the expression level of *TUB2*. Rt, roots; RL, rosette leaves; CL, cauline leaves; OF, open flowers; FB, flower buds; St, inflorescence stem; Sil, siliques. Error bars denote SD as described in Methods.

(B) to **(I)** Representative GUS staining of *J3:GUS* transgenic plants shows *J3* expression in a germinating seed collected 14 h **(B)** or 28 h **(C)** after stratification, a 3-d-old seedling **(D)**, a primary root **(E)**, a rosette leaf **(F)**, a cauline leaf **(G)**, an open flower **(H)**, and a silique **(I)**. Inset in **(D)** shows stronger *J3* expression in the shoot apex. Bars = 100 μm in **(B)**, **(C)**, and **(H)** and 500 μm in **(D)** to **(G)** and **(I)**.

(J) and **(K)** In situ localization of *J3* expression in a vegetative shoot apex of a 6-d-old plant **(J)** or a shoot apex of a 15-d-old plant during the floral transition **(K)**. The corresponding serial sections are shown in Supplemental Figure 4 online. For comparing signals, sections of shoot apices of 6- and 15-d-old plants were placed on the same slides for hybridization and detection. Bars = 25 μm.

plants were closely related to the levels of downregulation of *J3* expression (see Supplemental Figures 2C to 2E online), suggesting that downregulation of *J3* has a dosage-dependent effect on flowering. The strongest line, *AmiR-j3 #7*, which had the lowest level of *J3* expression, showed late flowering in both LDs and SDs as *j3-1* and *j3-2* (Figures 1D to 1G). In contrast with the significant late-flowering phenotype of *J3* loss-of-function mutants, transgenic plants overexpressing *J3* showed normal flowering time (see Supplemental Figure 3 online), implying that the excessive amount of *J3* might not affect flowering.

J3 Is Highly Expressed Throughout *Arabidopsis* Development

To examine the tissue expression pattern of *J3*, RT-PCR was performed using total RNA extracted from various tissues. *J3* was ubiquitously expressed in all the tissues examined with the lowest expression in flower buds (Figure 2A). To monitor the detailed tissue-specific expression pattern of *J3*, we generated a *J3:β-glucuronidase* (*GUS*) reporter construct in which the *J3* genomic fragment used for the gene complementation test (Figure 1H), but lacking the 3′ untranslated region, was fused to the *GUS* gene. Among 21 independent *J3:GUS* lines examined, 15 lines showed similar staining patterns. One representative line was selected for further detailed analysis of *J3* expression patterns. *J3:GUS* showed strong GUS staining in almost all the tissues examined (Figures 2B to 2I). Stronger J3:GUS signals were detected in the radical-hypocotyl transition zone of germinated seeds (Figures 2B and 2C), the vegetative shoot apex (Figure 2D), the basal part of cauline leaves (Figure 2G), the floral organs except petals (Figure 2H), and the basal and distal ends of siliques (Figure 2I).

In situ hybridization further revealed that *J3* was expressed in the vegetative shoot apex and emerging young leaves (Figure 2J) and upregulated in the shoot apex during the floral transition (Figure 2K; see Supplemental Figure 4 online). This observation is consistent with *J3* function in promoting flowering.

The Photoperiod, GA, and Vernalization Pathways Regulate *J3* Expression

To investigate how *J3* regulates flowering in response to various flowering signals, we examined *J3* expression in different environmental conditions and in a variety of flowering mutants. In wild-type Columbia (Col) plants grown under LDs, *J3* expression increased gradually before and during the floral transition occurring 9 to 13 d after germination and remained at high levels afterwards (see Supplemental Figure 5A online). On the contrary, *J3* was constantly expressed at lower levels under SDs within 18 d after germination, indicating an effect of the photoperiod pathway in promoting *J3* expression. We then performed daylength shift experiments to study the effect of photoperiod on *J3* expression. *J3* was rapidly induced upon daylength extension (Figure 3A), showing a pattern similar to that of *FT* expression (see Supplemental Figure 5B online) (Corbesier et al., 2007). Furthermore, *J3* expression exhibited a diurnal oscillation under LDs. These observations support that *J3* is regulated by the photoperiod pathway. However, *J3* expression was only slightly

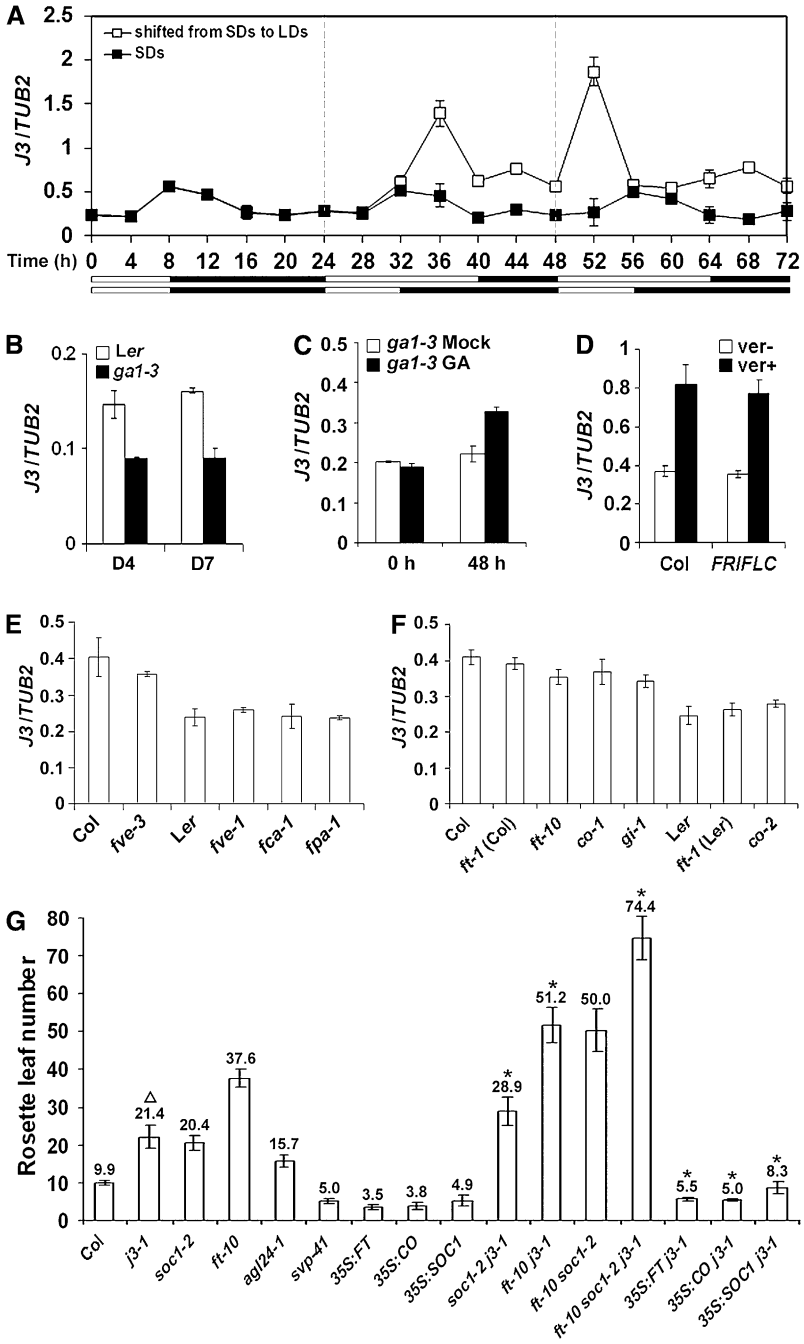

Figure 3. *J3* Is Regulated by the Photoperiod, Vernalization, and GA Pathways.

(A) *J3* expression in response to a SD to LD shift determined by quantitative real-time PCR. Wild-type Col seedlings were grown under SDs for 11 d before they were transferred to LDs. *J3* expression in these seedlings was examined at 4 h intervals for 3 d comprising one SD followed by two LDs, while its expression in plants grown under SDs was examined as a control. Bars below the graph indicate the duration of day (white) and night (black) for the shift experiment (top) and the control experiment (bottom). Error bars denote SD as described in Methods.

(B) Comparison of *J3* expression in the GA-deficient mutant *ga1-3* (*Ler* background) and wild-type L*er* plant determined by quantitative real-time PCR. Four-day-old (D4) and 7-d-old (D7) seedlings grown under SDs were harvested for expression analysis. Error bars denote SD as described in Methods. *J3* expression in **(B)** to **(F)** was normalized to *TUB2* expression.

(C) Effect of GA treatment on *J3* expression in *ga1-3* plants determined by quantitative real-time PCR. Exogenous GA (100 μM) or 0.1% ethanol (mock) was applied daily onto 3-week-old *ga1-3* seedlings grown under SDs for two consecutive days. *J3* expression was examined either before (0 h) or 48 h after (48 h) the first GA treatment. Error bars denote SD as described in Methods.

downregulated in loss-of-function mutants of two regulators in the photoperiod pathway, *FT* and *GIGANTEA*, in the Col background but not affected by another key regulator, *CONSTANS* (*CO*) (Figure 3F). Thus, the precise mechanism by which photoperiod modulates *J3* needs to be further elucidated. *J3* expression was consistently lower in the GA-deficient mutant *ga1-3* than in the wild-type plant grown under SDs (Figure 3B). Moreover, GA treatment for two consecutive days upregulated *J3* expression in *ga1-3* grown under SDs (Figure 3C), indicating that the GA pathway regulates *J3*. Similarly, *J3* expression was also upregulated in wild-type plants by vernalization treatment (Figure 3D). However, dramatic downregulation of *FLC* in *FRI FLC* after vernalization did not enhance the upregulation of *J3* in response to vernalization, indicating that vernalization regulates *J3* expression in an *FLC*-independent manner.

Like wild-type plants, *j3-1* exhibited similar levels of delayed flowering at 16°C versus 23°C (see Supplemental Figure 5C online), suggesting that *J3* is not directly involved in the thermosensory pathway. *J3* expression was also not affected in the various mutants of the autonomous pathway (Figure 3E), indicating that the autonomous pathway does not control *J3* expression. In addition, several other flowering-time regulators, such as *SOC1*, *AGAMOUS-LIKE24* (*AGL24*), and *SVP*, which mediate flowering signals from various genetic pathways, also did not affect *J3* expression (see Supplemental Figure 6 online). Taken together, these results suggest that *J3* perceives flowering signals from photoperiod, GA, and vernalization pathways but does not act downstream of floral pathway integrators (i.e., *SOC1* and *FT*).

We further analyzed the genetic interaction between *J3* and other flowering time genes that function downstream of multiple floral pathways (Figure 3G; see Supplemental Figure 7 online). A comparison of flowering time between *j3-1* and other flowering mutants demonstrated that the effect of *J3* on flowering in LDs and SDs was comparable to that of *SOC1*. Overexpression of *SOC1* or *FT* significantly suppressed the late-flowering phenotype of *j3-1* (Figure 3G), implying that these two major floral pathway integrators act either downstream of or in parallel with *J3*. Similarly, overexpression of *CO*, an upstream promoter of *FT* and *SOC1*, also significantly suppressed the *j3-1* phenotype. Either *ft-10* or *soc1-2* enhanced late flowering of *j3-1*, whereas *ft-10 soc1-2 j3-1* triple mutants exhibited much delayed flowering compared with single or double mutants (Figure 3G). These results indicate that besides the potential regulatory hierarchies among these genes, *J3*, *SOC1*, and *FT* also regulate flowering through other independent pathways.

J3 Interacts with SVP

The genetic interaction between *J3* and *FT* or *SOC1* and the initial identification of a J3 fragment as an interacting partner of SVP (Figures 1A and 1B) aroused our interest in further understanding the interaction between J3 and SVP, which is a direct transcriptional regulator of *FT* and *SOC1* (Lee et al., 2007; Li et al., 2008). To this end, we first compared the expression patterns of *J3* and *SVP* using their GUS reporter lines. There was a comparable spatial pattern of GUS staining in the aerial part of developing *J3:GUS* and *SVP:GUS* (Li et al., 2008) seedlings, although *J3:GUS* displayed much stronger GUS signals (Figure 4A). Second, we compared the subcellular localization of J3 and SVP in tobacco (*Nicotiana tabacum*) leaves using the red fluorescent protein (RFP) and green fluorescent protein (GFP) fusion constructs *35S:RFP-J3* and *35S:SVP-GFP*. Both RFP-J3 and SVP-GFP localized in the cytoplasm and nucleus, which is similar to the pattern observed for *35S:RFP* and *35S:GFP* (Figures 4B to 4E). To verify the subcellular localization of J3 and SVP in *Arabidopsis* cells, we then generated a functional *j3-1 gJ3-4HA* transgenic line (see Supplemental Figure 8A online) and the specific anti-SVP antibody (see Supplemental Figure 9 online). Immunoblot analyses revealed that J3 and SVP were present in both of the cytosolic and nuclear fractions of *j3-1 gJ3-4HA* and *35S:SVP* plants, respectively (see Supplemental Figures 8B and 8C online). These results demonstrate overlapping gene expression patterns and subcellular protein localization of *J3* and *SVP*.

Our yeast two-hybrid assay has shown that SVP interacts with the C-terminal region of J3 that contains both part of the zinc finger domain and the entire C-terminal domain (Figures 1A and 1B). To determine which domain is responsible for J3 interaction with SVP, we cloned the sequences of the zinc finger domain (J3-C1) and C-terminal domain (J3-C2), respectively, for further yeast two-hybrid assays (Figure 4F; see Supplemental Figure 10A online). The results demonstrated that the C-terminal domain of J3 was required for the interaction with SVP. On the contrary, none of the individual SVP domains (see Supplemental Figure 10B online) was sufficient for SVP interaction with J3 (Figure 4G; see Supplemental Figure 10C online). In vitro glutathione *S*-transferase (GST) pull-down assays further demonstrated that both GST-J3 and GST-J3-C2 could bind to in

Figure 3. (continued).

(D) Effect of vernalization treatment on *J3* expression determined by quantitative real-time PCR. For vernalization treatment, seeds were grown on MS medium and vernalized at 4°C under low-light conditions for 8 weeks. The 9-d-old seedlings grown under LDs were harvested for expression analysis. Error bars denote SD as described in Methods.

(E) *J3* expression determined by quantitative real-time PCR in 9-d-old mutants of the autonomous pathway. Error bars denote SD as described in Methods.

(F) *J3* expression determined by quantitative real-time PCR in 9-d-old mutants of the photoperiod pathway. Error bars denote SD as described in Methods.

(G) Flowering time of various mutants or transgenic plants (Col background) grown under LDs. Values were scored from at least 15 plants of each genotype. Mean values of rosette leaf number are indicated on top of bars. Error bars denote SD. Asterisks indicate significant difference in flowering time of plants with various genetic backgrounds compared with that of *j3-1* (Student's *t* test, $P < 0.05$). Open triangle indicates no statistically significant difference in flowering time of *j3-1* compared with that of *soc1-2* (Student's *t* test, $P > 0.5$).

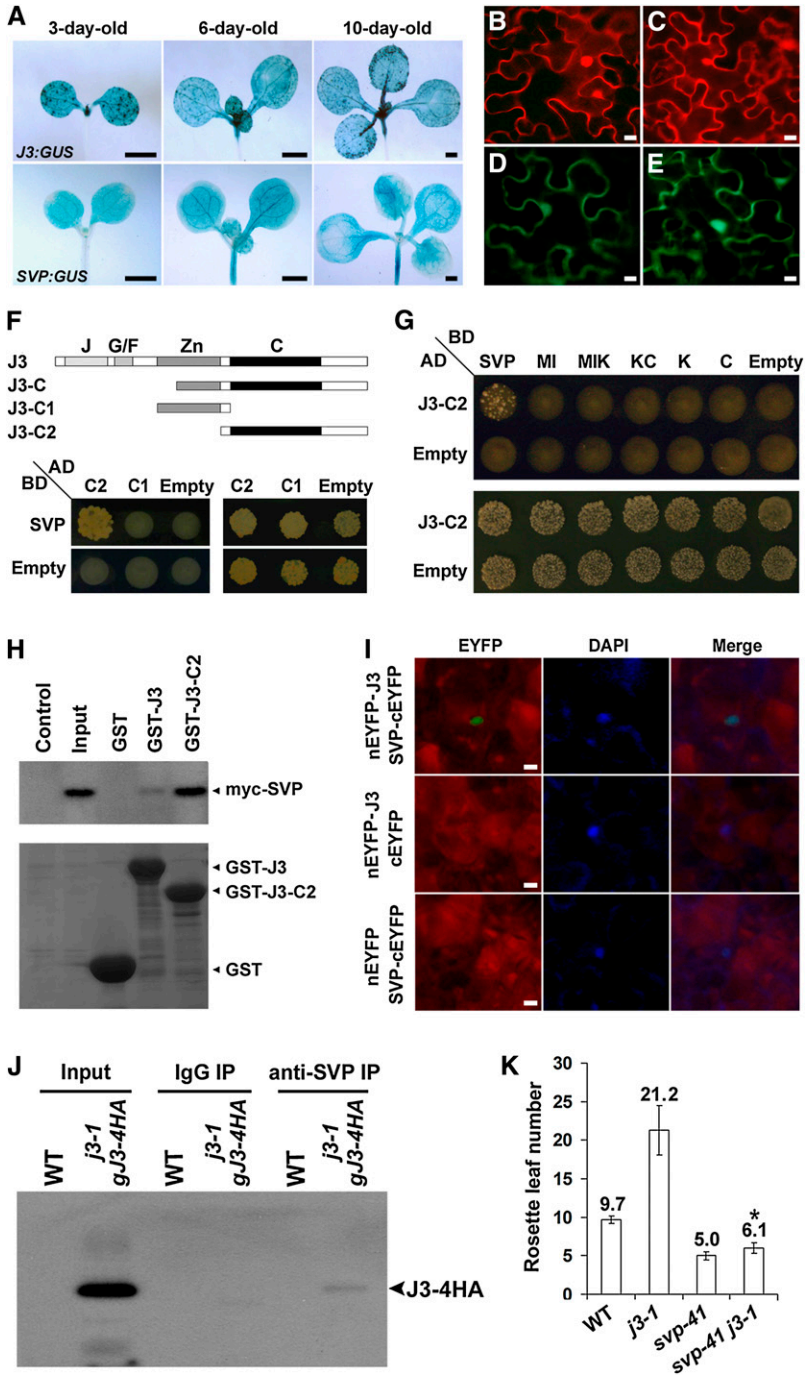

Figure 4. J3 Interacts with SVP.

(A) GUS staining of developing *J3:GUS* (top panels) and *SVP:GUS* seedlings. Bars = 1 mm.

(B) and **(C)** Subcellular localization of RFP-J3 in tobacco leaves. RFP localization was observed in tobacco leaves infiltrated with either *35S:RFP-J3* **(B)** or a *35S:RFP* control **(C)**. Bars = 10 μm.

(D) and **(E)** Subcellular localization of SVP-GFP in tobacco leaves. GFP localization was observed in tobacco leaves infiltrated with either *35S:SVP-GFP* **(D)** or a *35S:GFP* control **(E)**. Bars = 10 μm.

(F) Yeast two-hybrid assay of the interaction between SVP and J3-C1 or J3-C2. Top panel shows the schematic diagram of J3 truncated proteins that were fused to AD and used for yeast two-hybrid assays with SVP fused to BD. Transformed yeast cells were grown on SD/-Ade/-His/-Leu/-Trp medium (bottom left panel) and SD/-Leu/-Trp medium (bottom right panel). Empty refers to AD- or BD-containing vector only.

(G) Yeast two-hybrid assay of the interaction between J3-C2 and SVP truncated proteins. The schematic diagram of SVP truncated proteins is

vitro–translated full-length myc-SVP, while the affinity between GST-J3-C2 and myc-SVP was much stronger (Figure 4H). To test the in vivo interaction between J3 and SVP, we performed bimolecular fluorescence complementation (BiFC) experiments (Ohad et al., 2007), which monitors the protein–protein interaction through detecting the fluorescence signals emitted by reconstitution of an enhanced yellow fluorescent protein (EYFP) from two fragments (N- and C-terminal halves) fused to two interacting proteins. This revealed a direct interaction between J3 and SVP in the nuclei of living tobacco cells (Figure 4I). Furthermore, coimmunoprecipitation analysis of nuclear extracts from *j3-1 gJ3-4HA* confirmed the in vivo interaction of J3 and SVP in *Arabidopsis* (Figure 4J). These results provide evidence that J3 interacts with SVP in the nucleus.

We next examined the biological significance of the interaction of J3 and SVP through genetic analysis. As *J3* and *SVP* have opposite effects on the control of flowering time, *j3-1* and *svp-41* showed completely different flowering phenotypes (Figure 4K). However, *svp-41 j3-1* double mutants exhibited early flowering similar to *svp-41*, demonstrating that *SVP* is genetically epistatic to *J3*. This observation, together with the results showing in vitro and in vivo protein interaction of J3 and SVP, suggests that *J3* exerts its function in regulating flowering time via *SVP*.

J3 Regulates the Expression of *SOC1* and *FT*

Since *SVP* modulates flowering through transcriptional regulation of *SOC1* and *FT* (Lee et al., 2007; Li et al., 2008), we examined whether *J3* also affects *SOC1* and *FT* gene expression. First, we examined temporal expression of *SOC1* and *FT* in developing *j3-1* and wild-type seedlings. *FT* and *SOC1* expression was consistently reduced in developing *j3-1* seedlings at the vegetative phase and during the floral transition occurring from 9 d after germination (Figures 5A and 5B). Similar reduction of *FT* and *SOC1* expression was also observed in *AmiR-j3 #7* (see Supplemental Figure 11 online). On the contrary, the expression of *SVP* and *FLC*, the two potent transcriptional repressors of *FT* and *SOC1* (Helliwell et al., 2006; Searle et al., 2006; Lee et al., 2007; Li et al., 2008), remained unchanged in *j3-1* (see Supplemental Figure 12 online).

We further dissected developing seedlings before and during the floral transition (3 to 11 d old) to examine the spatial expression of *SOC1* and *FT* in the leaves (cotyledons and rosette leaves) and the aerial part without leaves (the shoot apical meristem and young leaf primordia). *SOC1* was consistently downregulated by 2- to 3- fold in the leaves and the aerial part without leaves in *j3-1* compared with wild-type plants (Figure 5C). *FT* expression was downregulated by up to 3-fold in *j3-1* leaves and was barely detectable in the aerial part without leaves in both *j3-1* and wild-type seedlings (Figure 5H). Furthermore, we examined GUS staining patterns of the established *SOC1:GUS* and *FT:GUS* transgenic lines (Takada and Goto, 2003; Liu et al., 2008) in the *j3-1* background. In agreement with the quantitative expression results (Figures 5C and 5H), SOC1:GUS signals were reduced both in the leaves and shoot apex of *j3-1* compared with wild-type plants (Figures 5D to 5G), while FT:GUS signals were also reduced in the vasculature of *j3-1* leaves (Figures 5I and 5J). These expression analyses, together with the genetic data (Figure 3G), support a regulatory hierarchy in which *J3* controls flowering through *FT* and *SOC1*.

Because two floral meristem identity genes, *AP1* and *LFY*, act downstream of *SOC1* and *FT*, we examined whether *J3* affects the expression of *AP1* and *LFY* during the floral transition. Indeed, we detected decreased expression of *AP1* and *LFY* in *j3-1* at 9 to 11 d after germination during which the floral transition starts (see Supplemental Figures 13A and 13B online).

Induction of *J3* Expression Immediately Activates *SOC1* and *FT*

To understand how *J3* regulates *SOC1* and *FT*, we created a *j3-1 pER22-J3* transgenic line in which overexpression of *J3* is controlled by an estradiol-inducible XVE system (Figure 6A) (Zuo et al., 2000). Application of β-estradiol to *j3-1 pER22-J3* was able to strongly activate *J3* expression within a short period. For example, in 9-d-old seedlings treated with β-estradiol, *J3* expression was immediately induced at 1 h after treatment and almost reached the maximum level at 4 h after treatment, which is comparable to its expression level in wild-type seedlings (Figure 6B). High expression levels of *J3* induced by β-estradiol could be maintained up to 24 h after treatment. Moreover, *j3-1 pER22-J3* plants grown on Murashige and Skoog (MS) medium supplemented with 10 μM β-estradiol flowered earlier than those subjected to mock treatment (Figure 6C), indicating that the

Figure 4. (continued).

illustrated in Supplemental Figure 10 online. Transformed yeast cells were grown on SD/-Ade/-His/-Leu/-Trp medium (top panel) and SD/-Leu/-Trp medium (bottom panel). AD, BD, and empty are as described above.

(H) In vitro GST pull-down assay with SVP and J3. Myc-tagged SVP protein generated by in vitro translation was incubated with immobilized GST, GST-J3, or GST-J3-C2. Immunoblot analysis was performed using anti-myc antibody. Control, in vitro translation product generated without a cDNA template. Input, 5% of the in vitro translation product. Arrowheads to right show expected sizes of GST and fusion proteins.

(I) BiFC analysis of the interaction between J3 and SVP. DAPI, fluorescence of 4',6-diamidino-2-phenylindole; Merge, merge of EYFP and DAPI. J3 and SVP were fused to nEYFP and cEYFP to generate nEYFP-J3 and SVP-cEYFP, respectively. A vector containing only nEYFP or cEYFP was used as a control. Bars = 10 μm.

(J) In vivo interaction between J3 and SVP shown by coimmunoprecipitation. Nuclear extracts from 9-d-old wild-type (WT) and *j3-1 gJ3-4HA* plants were incubated with preimmune serum (IgG) or anti-SVP antibody. The coimmunoprecipitated protein was detected by anti-HA antibody.

(K) Flowering phenotypes of *svp-41 j3-1*. Values were scored from at least 15 plants of each genotype. Mean values of rosette leaf number are indicated on top of bars. Error bars denote SD. Asterisk indicates no statistically significant difference in flowering time of *svp-41 j3-1* compared with that of *svp-41* (Student's *t* test, $P > 0.5$).

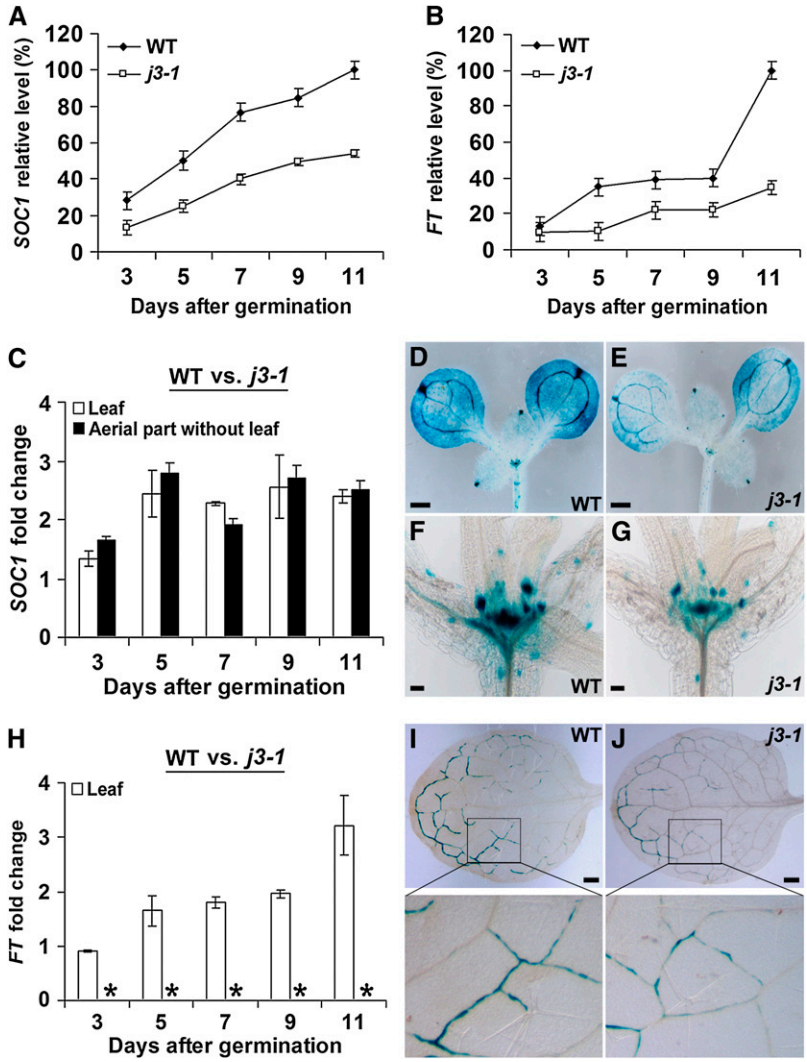

Figure 5. *SOC1* and *FT* Expression Is Regulated by *J3*.

(A) and **(B)** Temporal expression of *SOC1* **(A)** and *FT* **(B)** determined by quantitative real-time PCR in developing *j3-1* and wild-type (WT) seedlings under LDs. Error bars denote SD as described in Methods. The levels of gene expression normalized to *TUB2* expression are shown as relative values to the maximal expression level set at 100%.

(C) Fold change of *SOC1* expression determined by quantitative real-time PCR in leaves and the aerial part without leaves in the wild type against that in *j3-1* seedlings under LDs. *SOC1* expression was normalized to *TUB2* expression. Error bars denote SD as described in Methods.

(D) to **(G)** GUS staining of 9-d-old seedlings of *SOC1:GUS* (**[D]** and **[F]**) and *j3-1 SOC1:GUS* (**[E]** and **[G]**). **(D)** and **(E)** show GUS staining of the aerial part of the seedlings, while **(F)** and **(G)** show GUS staining in the shoot apex. Bars = 1 mm in **(D)** and **(E)** and 100 μm in **(F)** and **(G)**.

(H) Fold change of *FT* expression determined by quantitative real-time PCR in leaves and the aerial part without leaves in the wild type against that in *j3-1* seedlings under LDs. *FT* expression was normalized to *TUB2* expression. Asterisks indicate that *FT* transcript levels are barely detectable in the aerial part without leaves using quantitative real-time PCR. Error bars denote SD as described in Methods.

(I) and **(J)** GUS staining of the first true leaves of 11-d-old seedlings of *pFT:GUS* **(I)** and *j3-1 pFT:GUS* **(J)**. The bottom panels show a higher magnification of an area of the middle half of the leaves. Bars = 1 mm.

induced *J3* activity in *j3-1 pER22-J3* is biologically functional and responsible for promoting flowering. Using this established estradiol-inducible system, we tested the expression of *SOC1* and *FT* in response to induced *J3* expression (Figure 6D). *SOC1* and *FT* expression was immediately upregulated by *J3* within 4 h after β-estradiol treatment. After 4 h of treatment, *SOC1* and *FT* expression increased by 2.2- and 1.7-fold, respectively. Although the levels of upregulation slightly decreased afterwards, the expression of *SOC1* and *FT* remained upregulated up to 24 h after treatment. These observations suggest that *J3* modulates flowering time partly through activating the expression of two floral pathway integrators, *SOC1* and *FT*.

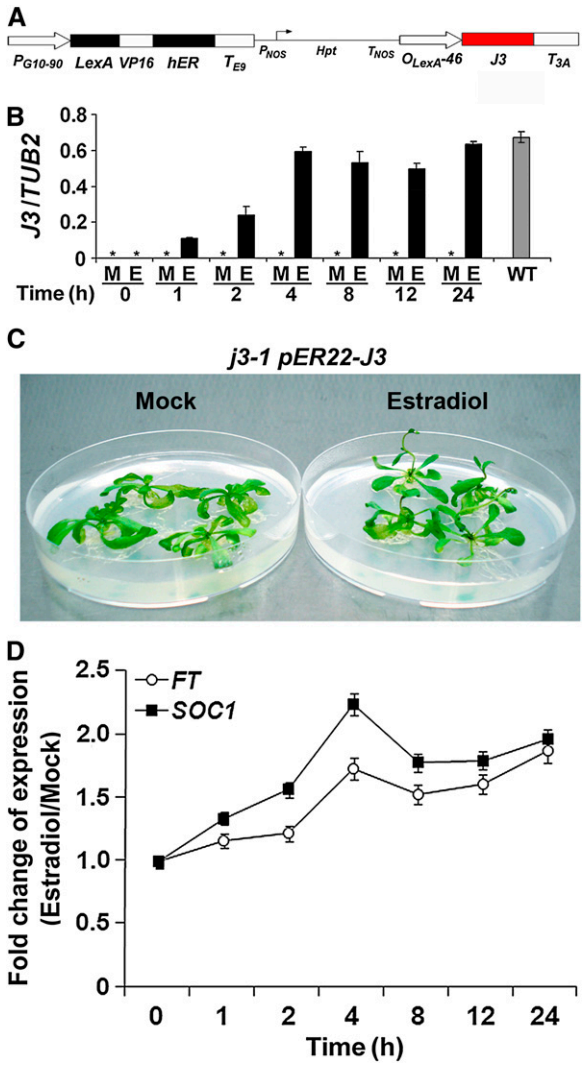

Figure 6. Upregulation of *SOC1* and *FT* upon Induction of *J3* Expression.

(A) Schematic diagram of the region between the right and left borders of the *pER22-J3* construct. *J3* cDNA fragment was inserted after eight copies of the LexA operator sequence fused to the −46 35S minimal promoter (O_{LexA}-*46*). Other components of *pER22* vector were described previously (Zuo et al., 2000; Liu et al., 2008).

(B) Induction of *J3* expression determined by quantitative real-time PCR in 9-d-old *j3-1 pER22-J3* transgenic seedlings mock treated (M) or treated with 10 μM β-estradiol (E) for 0, 1, 2, 4, 8, 12, and 24 h. *J3* expression in *j3-1 pER22-J3* induced by β-estradiol was compared with that in 9-d-old wild-type (WT) seedlings. Relative expression was normalized against *TUB2* expression. Asterisks indicate that quantitative real-time PCR analysis of *J3* RNA obtained very high Ct values because of its barely detectable level. Error bars denote SD as described in Methods.

(C) The estradiol-inducible *J3* system is biologically functional. The *j3-1 pER22-J3* plants treated daily with β-estradiol show earlier flowering than mock-treated plants.

(D) Fold change of induced *SOC1* and *FT* expression determined by quantitative real-time PCR in 9-d-old *j3-1 pER22-J3* seedlings treated with 10 μM β-estradiol relative to that in mock-treated seedlings. Relative expression was normalized against *TUB2* expression. Error bars denote SD as described in Methods.

J3 Activity Compromises SVP Binding to *SOC1* and *FT* Regulatory Regions

We further studied the molecular mechanism underlying which *J3* affects the expression of *SOC1* and *FT*. J3 does not possess a DNA binding domain. In addition, chromatin immunoprecipitation (ChIP) analysis using *j3-1 gJ3-4HA* revealed that J3 did not directly associate with the *SOC1* and *FT* genomic regions (see Supplemental Figure 14 online). Thus, *J3* might affect the expression of *SOC1* and *FT* by modulating the activity of their upstream transcription factors, such as SVP and FLC. Yeast two-hybrid and GST pull-down assays did not reveal direct interaction between J3 and FLC (see Supplemental Figure 15 online), whereas several lines of evidence in our study have demonstrated the physical and genetic interaction of J3 and SVP (Figure 4). In addition, a comparison of *SOC1* and *FT* expression in *j3-1* and *svp-41 j3-1* seedlings clearly showed that downregulation of *SOC1* and *FT* in *j3-1* was partly dependent on SVP activity (see Supplemental Figure 16 online). Based on these observations, we reasoned that J3 regulates *SOC1* and *FT* partly through SVP.

To elucidate how J3 modules SVP activity to modulate the expression of *SOC1* and *FT*, we first examined whether the protein abundance of SVP is affected by J3. To this end, we compared total SVP protein expression in either *gSVP-6HA* (Li et al., 2008) versus *j3-1 gSVP-6HA* or wild-type versus *j3-1* (see Supplemental Figures 17A and 17B online; *gSVP* represents the genomic fragment of *SVP*). In both cases, total SVP expression remained unchanged in the background of *j3-1*. We then measured nuclear SVP expression in both *gSVP-6HA* versus *j3-1 gSVP-6HA* and wild type versus *j3-1* and found that nuclear SVP expression was not altered in *j3-1* background (see Supplemental Figures 17A and 17B online). Furthermore, we established a *35S:SVP-GFP* transgenic line that showed late flowering (see Supplemental Figure 17C online), indicating that SVP-GFP retains the biological function of SVP. Using this line, we revealed that SVP subcellular localization remained unchanged in the wild-type or *j3-1* background. These results suggest that J3 does not affect nuclear SVP protein abundance and localization.

As SVP suppresses the transcription of *SOC1* and *FT* through direct binding to their regulatory regions, we next examined the effect of J3 on SVP binding to *SOC1* and *FT* by ChIP assays of two groups of plant materials, *gSVP-6HA* versus *j3-1 gSVP-6HA* and the wild type versus *j3-1*, using antihemagglutinin (HA) and anti-SVP antibodies, respectively. The abundance of the SVP-6HA protein in nuclear extracts (input) of *gSVP-6HA* and the corresponding immunoprecipitated fractions (eluate) used for ChIP assays was comparable to that in *j3-1 gSVP-6HA* after fixation (Figure 7A). ChIP assays showed that SVP-6HA was associated with the genomic regions near the number 6 fragment of *SOC1* and the number 8 fragment of *FT* with the highest enrichment fold, respectively (Figures 7C and 7D), which is consistent with the previous finding (Li et al., 2008). However, SVP binding to these regions was enhanced in *j3-1* background (Figure 7D), suggesting that loss of *J3* activity potentiates SVP binding to the regulatory sequences of its downstream genes. Furthermore, ChIP analysis of the wild type versus *j3-1* using anti-SVP antibody also demonstrated the enhanced binding of endogenous SVP to the identical genomic regions identified by

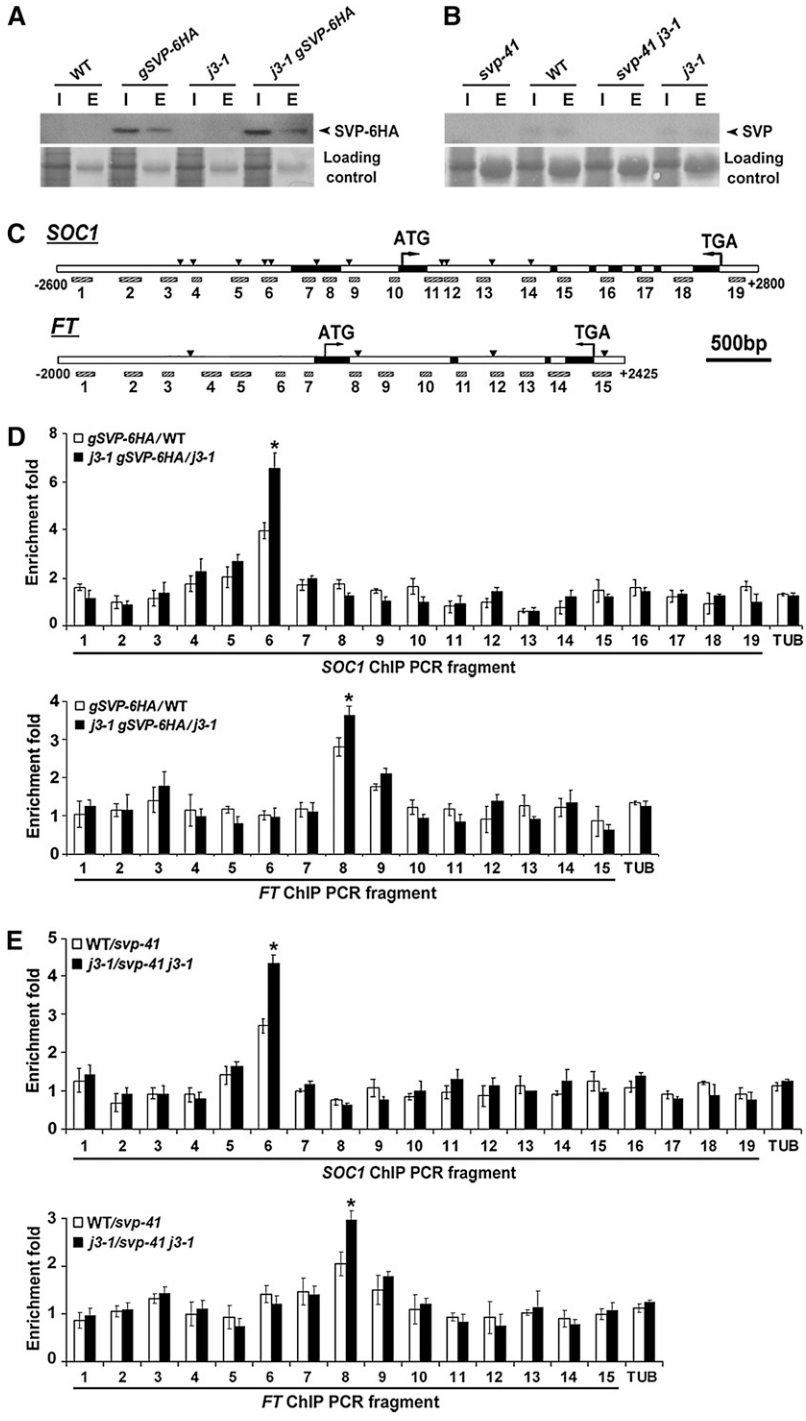

Figure 7. Loss of *J3* Activity Enhances SVP Binding to *SOC1* and *FT* Regulatory Regions.

(A) Measurement of SVP-6HA protein abundance in nuclear extracts or immunoprecipitated fractions of 9-d-old *gSVP-6HA* and *j3-1 gSVP-6HA* seedlings. Nuclear extracts from various plants served as the input (I), while immunoprecipitated fractions by anti-HA antibody were used as the eluate (E). Immunoblot analysis was performed using anti-HA antibody. WT, wild type.

(B) Measurement of SVP protein abundance in nuclear extracts or immunoprecipitated fractions of 9-d-old wild-type and *j3-1* seedlings. Nuclear extracts from various plants served as the input (I), while immunoprecipitated fractions by anti-SVP antibody were used as the eluate (E). Immunoblot analysis was performed using anti-SVP antibody.

(C) Schematic diagrams show the *SOC1* (top panel) and *FT* (bottom panel) genomic regions. Exons are represented by black boxes, while introns and

ChIP analysis of *gSVP-6HA* in the absence of *J3* activity (Figures 7B, 7C, and 7E). These results, together with the fact that J3 activity promotes the expression of *SOC1* and *FT*, suggest that *J3* regulates flowering time, at least in part, through compromising SVP binding to the regulatory regions of *SOC1* and *FT*.

We further examined the capacity of SVP binding in response to induced *J3* activity using the established functional estradiol-inducible system (*j3-1 pER22-J3*) (Figures 6A to 6C). To this end, ChIP analyses were performed on 9-d-old *j3-1 pER22-J3* seedlings treated with 10 μM β-estradiol for 4 h, in which *J3* expression was induced to a similar level as that in wild-type seedlings (Figure 6B). The abundance of endogenous SVP in nuclear extracts (input) of *j3-1* and *j3-1 pER22-J3* mock treated or treated with β-estradiol and in their corresponding immunoprecipitated fractions (eluate) used for ChIP assays was almost comparable (Figure 8A), suggesting that both estradiol treatment and the resulting change in *J3* expression do not affect SVP expression in the nucleus. Estradiol treatment of *j3-1* did not affect SVP binding to the genomic regions near the number 6 fragment of *SOC1* and the number 8 fragment of *FT*, respectively (Figures 8B and 8C). However, estradiol treatment of *j3-1 pER22-J3*, which induced *J3* expression, decreased SVP binding to these regions (Figures 8B and 8C). These results demonstrate that induced *J3* activity is able to rapidly compromise SVP binding capacity in planta.

DISCUSSION

Intensive studies of flowering in *Arabidopsis* have identified a number of regulators involved in the dynamic process of the floral transition in response to various environmental and developmental cues perceived by several flowering genetic pathways. A group of MADS box transcription factors, such as *FLC*, *SVP*, *SOC1*, and *AGL24* (Michaels and Amasino, 1999; Hartmann et al., 2000; Lee et al., 2000; Yu et al., 2002; Michaels et al., 2003), act as essential regulators at the convergence point of multiple flowering pathways. They integrate flowering signals and further regulate the spatial and temporal expression of floral meristem identity genes to determine the transition from vegetative shoot apical meristems to inflorescence meristems. Among these MADS box regulators, SVP serves as a central flowering repressor that functions together with another potent repressor, FLC, in maintaining the duration of the vegetative phase by repressing the expression of two major floral pathway integrators, *FT* and *SOC1* (Hartmann et al., 2000; Lee et al., 2007; Li et al., 2008). Previous studies have suggested that various flowering pathways promote flowering through regulating either *SVP* mRNA abundance or SVP protein abundance. The flowering signals perceived by the thermosensory, autonomous, and GA pathways suppress *SVP* expression (Lee et al., 2007; Li et al., 2008). Although the photoperiod pathway does not affect *SVP* expression, two essential circadian clock components, *LATE ELONGATED HYPOCOTYL* and *CIRCADIAN CLOCK ASSOCIATED1*, regulate the abundance of SVP protein under continuous light (Fujiwara et al., 2008). In this study, we report a flowering regulator, J3, which promotes flowering through attenuating SVP binding to the regulatory sequences of *FT* and *SOC1* rather than affecting the abundance of *SVP* mRNA or protein (Figure 8D).

Several lines of evidence have demonstrated that J3 is an essential regulator that is required for the integration of flowering signals. First, the late-flowering phenotype of *J3* loss-of-function mutants in both LDs and SDs is similar to or even more significant than that exhibited by loss of function of other key flowering promoters, such as *SOC1* and *AGL24* (Figure 3; see Supplemental Figure 7 online). Second, *J3* expression is regulated by photoperiod, GA, and vernalization pathways (Figure 3), indicating that it affects flowering in response to both environmental and developmental cues. Third, J3 interacts directly with SVP and attenuates its in vivo binding to the regulatory sequences of *SOC1* and *FT* in developing seedlings (Figures 4 and 7). The effect of J3 activity on SVP binding capacity is closely related to *SOC1* and *FT* expression in either *j3* mutants or *j3-1 pER22-J3* in which *J3* expression is induced (Figures 5 to 8). These observations support that J3 acts an important regulator mediating the floral transition through SVP. This is consistent with the genetic evidence showing that *svp-41* greatly suppresses the late-flowering phenotype of *j3-1* (Figure 4K). As SVP functions as a dosage-dependent repressor of flowering (Hartmann et al., 2000), modulation of its activity by increased J3 activity in response to multiple flowering signals emerges as another important mechanism for promoting the transition from vegetative to reproductive growth in *Arabidopsis*.

Although our data support that J3 promotes flowering largely through its interaction with SVP and regulation of *SOC1* and *FT*, there is evidence indicating that J3-mediated flowering process involves other unknown regulators. The expression of *SOC1* and *FT* in *svp-41 j3-1* was different from that in *svp-41* (see Supplemental Figure 16 online), implying that regulation of *SOC1* and *FT* by J3 is not merely through SVP. Furthermore, J3 likely promotes flowering through other pathways independently of *SOC1* and *FT*. This is supported by two pieces of evidence. First, *ft-10 soc1-2*

Figure 7. (continued).

upstream regions are represented by white boxes. Bent arrows denote translation start sites and stop codons. Arrowheads indicate the sites containing either single mismatch or perfect match to the consensus binding sequence (CArG box) of MADS domain proteins. Nineteen and fifteen DNA fragments spanning the *SOC1* and *FT* genomic regions were examined by ChIP enrichment test as shown in **(D)** and **(E)**, respectively.

(D) ChIP analysis of SVP-6HA binding to the regulatory regions of *SOC1* (top panel) and *FT* (bottom panel) in *gSVP-6HA* and *j3-1 gSVP-6HA*. ChIP analysis was performed using the input and eluate described in **(A)**.

(E) ChIP analysis of SVP binding to the regulatory regions of *SOC1* (top panel) and *FT* (bottom panel) in the wild type and *j3-1*. ChIP analysis was performed using the input and eluate described in **(B)**.

A *TUB2* fragment was amplified as a negative control in **(D)** and **(E)**. Significant differences of enrichment fold changes in comparison with respective controls are indicated with asterisks (Student's *t* test, $P < 0.05$). Error bars denote SD of triplicate assays.

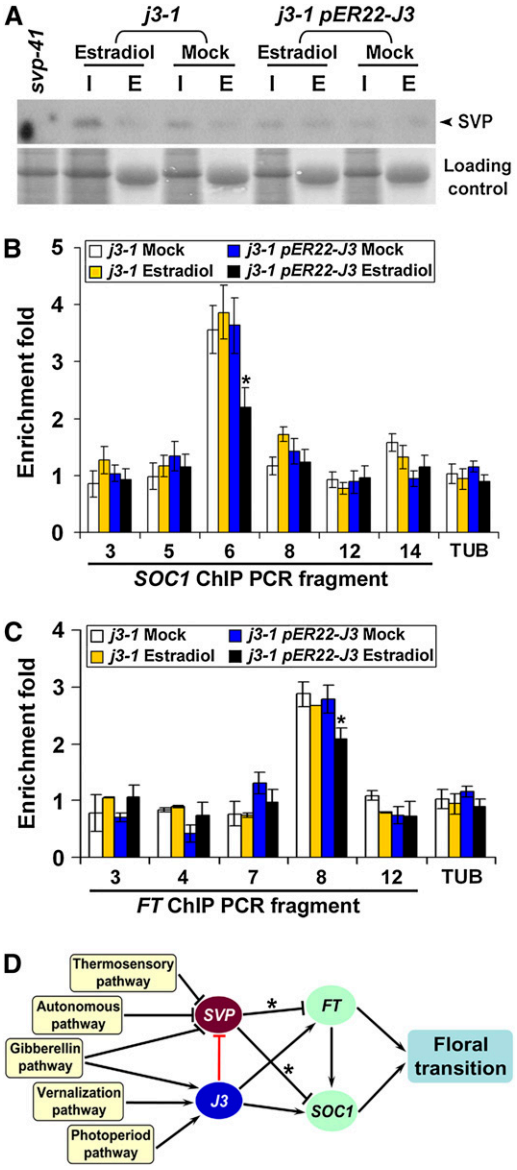

Figure 8. J3 Regulates Flowering Time by Mediating SVP Activity to Regulate *SOC1* and *FT* Transcription.

(A) Measurement of SVP protein abundance in nuclear extracts or immunoprecipitated fractions of 9-d-old *j3-1* and *j3-1 pER22-J3* seedlings mock treated or treated with 10 μM β-estradiol for 4 h. Nuclear extracts from various plants served as the input (I), while immunoprecipitated fractions by anti-SVP antibody were used as the eluate (E). Immunoblot analysis was performed using anti-SVP antibody.

(B) and **(C)** ChIP analysis of SVP binding to the regulatory regions of *SOC1* **(B)** and *FT* **(C)** upon induced expression of *J3* in 9-d-old *j3-1 pER22-J3* seedlings. ChIP analysis was performed using the input and eluate described in **(A)**. The DNA fragments amplified in ChIP assays are illustrated in Figure 7C. A *TUB2* fragment was amplified as a negative control. Significant differences of enrichment fold changes in comparison with respective controls are indicated with asterisks (Student's *t* test, $P < 0.05$). Error bars denote SD of triplicate assays.

(D) Proposed model of *J3* function in mediating the integration of flowering signals during the floral transition. *J3* expression is promoted by the photoperiod, vernalization, and GA pathways. *J3* promotes flowering partly through upregulating the expression of *SOC1* and *FT*. J3 interacts with SVP in the nucleus and attenuates SVP binding to the regulatory sequences of *SOC1* and *FT*, thus affecting their expression. Stimulatory interactions are indicated by arrows, while repressive interactions are indicated by T-bars. Asterisks indicate the confirmed direct transcriptional regulation.

j3-1 flowers much later than any single or double mutants (Figure 3G), suggesting that another regulator(s) contributes to J3-mediated flowering in parallel with *SOC1* and *FT*. Second, while the genetic result shows that *svp-41* greatly suppresses *j3-1* (Figure 4K), the upregulation of *SOC1* and *FT* in *svp-41 j3-1* was less than that in *svp-41* (see Supplemental Figure 16 online), implying that the interaction between J3 and SVP also controls other downstream regulators in addition to *SOC1* and *FT*.

A large number of J-domain proteins, which are traditionally considered as molecular chaperones along with Hsp70, have been identified in both prokaryotes and eukaryotes (Craig et al., 2006).The *Arabidopsis* genome contains 120 J-domain proteins, and their functions are mostly uncharacterized (Miernyk, 2001; Rajan and D'Silva, 2009). While many studies have proposed that J-domain proteins are part of chaperone machineries involved in maintaining protein homeostasis under environmental stress conditions, our results have shed light on the identity of J-domain proteins as transcriptional regulators that play an indispensable role in mediating plant development. Interestingly, MADS domain proteins, including SVP, are also a group of conserved transcription factors that determine developmental processes and signal transduction in eukaryotes (Riechmann and Meyerowitz, 1997; Theissen, 2000; Ng and Yanofsky, 2001). Therefore, the interaction between J3 and SVP revealed in this study may represent an emerging molecular relationship between their respective families of conserved regulators, which links fundamental cellular homeostasis in response to environmental stimuli and developmental control in eukaryotes.

METHODS

Plant Materials and Growth Conditions

Arabidopsis thaliana ecotypes Col-0 or Landsberg *erecta* (L*er*) were grown on soil or MS plates under LDs (16 h light/8 h dark) or SDs (8 h light/16 h dark) at 23°C ± 2°C. The mutants *co-1*, *gi-1*, *ft-1* (L*er ft-1* introgressed into Col), *ft-10*, *fve-3*, *soc1-2*, *agl24-1*, *svp-41*, *j3-1*, and *j3-2* are in the Col background, while *co-2*, *ft-1*, *fve-1*, *fca-1*, *fpa-1*, and *ga1-3* are in the L*er* background (Li et al., 2008). All transgenic plants were generated in the Col background through *Agrobacterium tumefaciens*–mediated transformation. Except for the transformants harboring *pER22-J3* that were selected on MS medium supplemented with hygromycin, transgenic plants with other constructs were selected by Basta on soil. β-Estradiol induction of *j3-1 pER22-J3* plants was performed as previously described (Liu et al., 2008).

Plasmid Construction

For the complementation test, a 4.5-kb *J3* genomic fragment (*gJ3*) including 2.2-kb upstream sequence, 1.9-kb coding sequence plus introns, and 0.4-kb 3′ untranslated region was amplified using primers

gJ3-F-*Pst*I (5′-AACTGCAGCCAACCTACTTGCATGTTAACAAG-3′) and gJ3-R-*Xma*I (5′-CCCCCCGGGGTACATGTCATCGGAGTTAACAC-3′). The resulting PCR fragment was digested and cloned into pHY105 (Liu et al., 2007). To construct *gJ3-4HA*, the *J3* genomic fragment including 2.2-kb upstream sequence and 1.9-kb coding sequence plus introns was amplified with primers gJ3-F-*Pst*I and gJ3-R2-*Xma*I (5′-CCCCCCGGG-CTGCTGGGCACATTGCACCC-3′) and cloned into pGreen-4HA to obtain an in-frame fusion of J3-4HA. The pGreen-6HA vector (Li et al., 2008) was cut with *Bam*HI and self-ligated to generate pGreen-4HA. To construct *J3:GUS*, the *J3* genomic region was amplified with primers gJ3-F-*Pst*I and gJ3-R2-*Xma*I and cloned into pHY107 (Liu et al., 2007). To construct *AmiR-j3*, design of the AmiR was performed using the software on the website (http://wmd2.weigelworld.org). Based on the *J3* sequence, a set of four primers was generated and used for the PCR amplification according to the published protocol (Schwab et al., 2006). The resulting PCR fragment was digested with *Eco*RI and *Bam*HI and cloned into pGreen 0229-35S vector (Yu et al., 2004). To construct *pER22-J3* and *35S:J3*, the *J3* cDNA sequence was amplified and cloned into pER22 (Liu et al., 2008) and pGreen 0229-35S (Yu et al., 2004) vectors, respectively.

Expression Analysis

Total RNA was extracted using RNeasy plant mini kit (Qiagen) and reverse transcribed with the SuperScript III first-strand synthesis system (Invitrogen) according to the manufacturer's instructions. Quantitative real-time PCR was performed using three biological replicates with three technical replicates each on 7900HT Fast real-time PCR systems with SYBR Green PCR Master Mix (Applied Biosystems). The mean and SD were determined from one representative biological replicate. The relative expression levels were determined as previously described (Li et al., 2008). The difference between the cycle threshold (Ct) of target genes and the Ct of control primers ($\Delta Ct = Ct_{target\ gene} - Ct_{control}$) was used to obtain the normalized expression of target genes. RT-PCR, nonradioactive in situ hybridization, and synthesis of RNA probes were performed as previously described (Yu et al., 2002). Primers used for gene expression analysis are listed in Supplemental Table 1 online. For *J3:GUS* reporter construct, we checked 17 independent transgenic lines at the T3 generation and selected one representative line for further analysis. GUS staining was performed as previously described (Yu et al., 2000).

Yeast Two-Hybrid Assay

To construct the vectors for yeast two-hybrid assays, the coding regions of SVP and J3 and their truncated versions were amplified and cloned into pGADT7 or pGBKT7 (Clontech). The yeast two-hybrid assay was performed using the Yeastmaker Yeast Transformation System 2 according to the manufacturer's instructions (Clontech). The library screening was performed as previously described (Liu et al., 2009b).

In Vitro GST Pull-Down Assay

The cDNAs encoding J3 and J3-C2 were cloned into pGEX-6p-2 vector (Pharmacia). The GST-J3 and GST-J3-C2 fusion proteins were produced by inducing *Escherichia coli* BL21 cells harboring the corresponding constructs with isopropyl β-D-1-thiogalactopyranoside at 16°C. The soluble GST fusion proteins were extracted and immobilized on glutathione sepharose beads (Amersham Biosciences) for subsequent pull-down assays. Myc-tagged SVP proteins were generated as previously described (Li et al., 2008). To produce myc-tagged FLC proteins, the full-length *FLC* cDNA was cloned into the pGBKT7 (Clontech). The resulting plasmid was added to the TNT T7 Quick Coupled Transcription/Translation Systems (Promega) to synthesize myc-FLC. These epitope-tagged proteins were incubated with the immobilized GST and GST fusion proteins. Proteins retained on the beads were resolved by SDS-PAGE and detected with anti-myc antibody (Santa Cruz Biotechnology).

BiFC Analysis

The full-length coding regions of *SVP* and *J3* were cloned into primary pSAT1 vectors. The resulting cassettes including fusion proteins and the constitutive promoters were cloned into pHY105 and transformed into *Agrobacterium*. The *Agrobacteria* were coinfiltrated into 3-week-old tobacco (*Nicotiana benthamiana*) leaves as previously described (Sparkes et al., 2006).

Production of SVP-Specific Antibody

Synthetic peptides corresponding to amino acid residues 218 to 233 of the SVP protein (STGAPVDSESSDTSLR) (Fujiwara et al., 2008) were used to produce polyclonal rabbit antibodies (GenScript). Anti-SVP antibody could specifically detect endogenous SVP but not the closest homolog of SVP, AGL24 (see Supplemental Figure 9 online).

Coimmunoprecipitation Experiment

Wild-type and *j3-1 gJ3-4HA* plants were ground with mortar and pestle in liquid nitrogen, and nuclear proteins were extracted as previously described (Liu et al., 2009b). The protein extracts were then incubated with Protein G PLUS-Agarose (Santa Cruz Biotechnology) and anti-SVP antibody or preimmune serum at 4°C for 2 h. The immunoprecipitated proteins and the protein extracts as inputs were resolved by SDS-PAGE and detected by anti-HA antibody (Santa Cruz Biotechnology).

ChIP Assay

Seedlings were fixed on ice for 40 min in 1% formaldehyde under vacuum. Fixed tissues were homogenized. Chromatin was isolated and sonicated to produce DNA fragments of ~250 bp. SVP-6HA and endogenous SVP protein were immunoprecipitated by anti-HA agarose conjugate (Sigma-Aldrich) and anti-SVP antibody bound to Protein G PLUS Agarose, respectively. Relative enrichment of each fragment was determined by quantitative real-time PCR as previously reported (Li et al., 2008). Primer pairs used for ChIP assays are listed in Supplemental Table 1 online. All ChIP assays were repeated three times with similar results, and representative data are presented in Figures 7 and 8.

Accession Numbers

Sequence data from this article can be found in the Arabidopsis Genome Initiative under the following accession numbers: *J3* (At3g44110), *J2* (At5g22060), *SVP* (At2g22540), *FT* (At1g65480), *SOC1* (At2g45660), *FLC* (At5g10140), and *TUB2* (At5g62690). The T-DNA insertion mutants *j3-1* (Salk_132923) and *j3-2* (Salk_141625) were provided by TAIR.

Supplemental Data

The following materials are available in the online version of this article.

Supplemental Figure 1. The Amino Acid Sequence of J3 Is Highly Conserved among Eukaryotes.

Supplemental Figure 2. Downregulation of *J3* Expression Delays Flowering.

Supplemental Figure 3. Overexpression of *J3* Does Not Significantly Affect Flowering.

Supplemental Figure 4. In Situ Localization of *J3* Expression in Serial Sections of Vegetative Shoot Apices or Shoot Apices during the Floral Transition.

Supplemental Figure 5. Regulation of *J3* by Various Flowering Genetic Pathways.

Supplemental Figure 6. *AGL24*, *SOC1*, and *SVP* Do Not Affect *J3* Expression.

Supplemental Figure 7. Flowering Time of Various Mutants (Col Background) Grown under Short Days.

Supplemental Figure 8. Subcellular Localization of J3 and SVP Revealed by Immunoblot Analysis.

Supplemental Figure 9. Anti-SVP Antibody Specifically Detects SVP.

Supplemental Figure 10. The Interaction between J3 and SVP Requires the C-Terminal Domain of J3 and Full-Length SVP Protein.

Supplemental Figure 11. Expression of *SOC1* and *FT* in *AmiR-j3* Seedlings.

Supplemental Figure 12. *J3* Does Not Affect the Expression of *SVP* and *FLC*.

Supplemental Figure 13. The Expression of *AP1* and *LFY* Is Regulated by *J3*.

Supplemental Figure 14. J3 Is Not Associated with the *SOC1* and *FT* Genomic Regions.

Supplemental Figure 15. J3 Does Not Interact with FLC.

Supplemental Figure 16. A Comparison of *SOC1* and *FT* Expression in *j3-1*, *svp-41*, and *svp-41 j3-1* Seedlings.

Supplemental Figure 17. J3 Does Not Affect Total and Nuclear SVP Protein Expression or SVP-GFP Subcellular Localization.

Supplemental Table 1. List of Primers Used in This Study.

ACKNOWLEDGMENTS

We thank K. Goto, D. Weigel, P. Huijser, I. Lee, R. Amasino, M.F. Yanofsky, and the ABRC for materials. This work was supported by Academic Research Fund T208B3113 from the Ministry of Education, Singapore, and intramural research funds from Temasek Life Sciences Laboratory.

Received January 7, 2011; revised January 7, 2011; accepted February 8, 2011; published February 22, 2011.

REFERENCES

Blázquez, M.A., Ahn, J.H., and Weigel, D. (2003). A thermosensory pathway controlling flowering time in *Arabidopsis thaliana*. Nat. Genet. **33:** 168–171.

Blázquez, M.A., and Weigel, D. (2000). Integration of floral inductive signals in Arabidopsis. Nature **404:** 889–892.

Boss, P.K., Bastow, R.M., Mylne, J.S., and Dean, C. (2004). Multiple pathways in the decision to flower: enabling, promoting, and resetting. Plant Cell **16** (suppl.): S18–S31.

Bukau, B., and Horwich, A.L. (1998). The Hsp70 and Hsp60 chaperone machines. Cell **92:** 351–366.

Caplan, A.J., Cyr, D.M., and Douglas, M.G. (1993). Eukaryotic homologues of *Escherichia coli* dnaJ: A diverse protein family that functions with hsp70 stress proteins. Mol. Biol. Cell **4:** 555–563.

Corbesier, L., Vincent, C., Jang, S., Fornara, F., Fan, Q., Searle, I., Giakountis, A., Farrona, S., Gissot, L., Turnbull, C., and Coupland, G. (2007). FT protein movement contributes to long-distance signaling in floral induction of Arabidopsis. Science **316:** 1030–1033.

Craig, E.A., Huang, P., Aron, R., and Andrew, A. (2006). The diverse roles of J-proteins, the obligate Hsp70 co-chaperone. Rev. Physiol. Biochem. Pharmacol. **156:** 1–21.

Cyr, D.M., Langer, T., and Douglas, M.G. (1994). DnaJ-like proteins: Molecular chaperones and specific regulators of Hsp70. Trends Biochem. Sci. **19:** 176–181.

de Crouy-Chanel, A., Kohiyama, M., and Richarme, G. (1995). A novel function of *Escherichia coli* chaperone DnaJ. Protein-disulfide isomerase. J. Biol. Chem. **270:** 22669–22672.

Fujiwara, S., Oda, A., Yoshida, R., Niinuma, K., Miyata, K., Tomozoe, Y., Tajima, T., Nakagawa, M., Hayashi, K., Coupland, G., and Mizoguchi, T. (2008). Circadian clock proteins LHY and CCA1 regulate SVP protein accumulation to control flowering in *Arabidopsis*. Plant Cell **20:** 2960–2971.

Georgopoulos, C. (1992). The emergence of the chaperone machines. Trends Biochem. Sci. **17:** 295–299.

Georgopoulos, C.P., Lundquist-Heil, A., Yochem, J., and Feiss, M. (1980). Identification of the *E. coli* dnaJ gene product. Mol. Gen. Genet. **178:** 583–588.

Goffin, L., and Georgopoulos, C. (1998). Genetic and biochemical characterization of mutations affecting the carboxy-terminal domain of the *Escherichia coli* molecular chaperone DnaJ. Mol. Microbiol. **30:** 329–340.

Ham, B.K., Park, J.M., Lee, S.B., Kim, M.J., Lee, I.J., Kim, K.J., Kwon, C.S., and Paek, K.H. (2006). Tobacco Tsip1, a DnaJ-type Zn finger protein, is recruited to and potentiates Tsi1-mediated transcriptional activation. Plant Cell **18:** 2005–2020.

Hartmann, U., Höhmann, S., Nettesheim, K., Wisman, E., Saedler, H., and Huijser, P. (2000). Molecular cloning of SVP: A negative regulator of the floral transition in Arabidopsis. Plant J. **21:** 351–360.

Helliwell, C.A., Wood, C.C., Robertson, M., James Peacock, W., and Dennis, E.S. (2006). The Arabidopsis FLC protein interacts directly in vivo with SOC1 and FT chromatin and is part of a high-molecular-weight protein complex. Plant J. **46:** 183–192.

Kardailsky, I., Shukla, V.K., Ahn, J.H., Dagenais, N., Christensen, S.K., Nguyen, J.T., Chory, J., Harrison, M.J., and Weigel, D. (1999). Activation tagging of the floral inducer FT. Science **286:** 1962–1965.

Kneissl, J., Wachtler, V., Chua, N.H., and Bolle, C. (2009). OWL1: An *Arabidopsis* J-domain protein involved in perception of very low light fluences. Plant Cell **21:** 3212–3225.

Kobayashi, Y., Kaya, H., Goto, K., Iwabuchi, M., and Araki, T. (1999). A pair of related genes with antagonistic roles in mediating flowering signals. Science **286:** 1960–1962.

Lee, H., Suh, S.S., Park, E., Cho, E., Ahn, J.H., Kim, S.G., Lee, J.S., Kwon, Y.M., and Lee, I. (2000). The AGAMOUS-LIKE 20 MADS domain protein integrates floral inductive pathways in Arabidopsis. Genes Dev. **14:** 2366–2376.

Lee, J.H., Yoo, S.J., Park, S.H., Hwang, I., Lee, J.S., and Ahn, J.H. (2007). Role of SVP in the control of flowering time by ambient temperature in Arabidopsis. Genes Dev. **21:** 397–402.

Li, D., Liu, C., Shen, L., Wu, Y., Chen, H., Robertson, M., Helliwell, C.A., Ito, T., Meyerowitz, E., and Yu, H. (2008). A repressor complex governs the integration of flowering signals in Arabidopsis. Dev. Cell **15:** 110–120.

Liberek, K., Marszalek, J., Ang, D., Georgopoulos, C., and Zylicz, M. (1991). *Escherichia coli* DnaJ and GrpE heat shock proteins jointly stimulate ATPase activity of DnaK. Proc. Natl. Acad. Sci. USA **88:** 2874–2878.

Liu, C., Chen, H., Er, H.L., Soo, H.M., Kumar, P.P., Han, J.H., Liou, Y. C., and Yu, H. (2008). Direct interaction of AGL24 and SOC1 integrates flowering signals in Arabidopsis. Development **135:** 1481–1491.

Liu, C., Thong, Z., and Yu, H. (2009a). Coming into bloom: The specification of floral meristems. Development **136:** 3379–3391.

Liu, C., Xi, W., Shen, L., Tan, C., and Yu, H. (2009b). Regulation of floral patterning by flowering time genes. Dev. Cell **16:** 711–722.

Liu, C., Zhou, J., Bracha-Drori, K., Yalovsky, S., Ito, T., and Yu, H. (2007). Specification of Arabidopsis floral meristem identity by repression of flowering time genes. Development **134:** 1901–1910.

Michaels, S.D., and Amasino, R.M. (1999). FLOWERING LOCUS C encodes a novel MADS domain protein that acts as a repressor of flowering. Plant Cell **11:** 949–956.

Michaels, S.D., Ditta, G., Gustafson-Brown, C., Pelaz, S., Yanofsky, M., and Amasino, R.M. (2003). AGL24 acts as a promoter of flowering in Arabidopsis and is positively regulated by vernalization. Plant J. **33:** 867–874.

Miernyk, J.A. (2001). The J-domain proteins of *Arabidopsis thaliana*: An unexpectedly large and diverse family of chaperones. Cell Stress Chaperones **6:** 209–218.

Mouradov, A., Cremer, F., and Coupland, G. (2002). Control of flowering time: interacting pathways as a basis for diversity. Plant Cell **14** (suppl.): S111–S130.

Ng, M., and Yanofsky, M.F. (2001). Function and evolution of the plant MADS-box gene family. Nat. Rev. Genet. **2:** 186–195.

Ohad, N., Shichrur, K., and Yalovsky, S. (2007). The analysis of protein-protein interactions in plants by bimolecular fluorescence complementation. Plant Physiol. **145:** 1090–1099.

Qiu, X.B., Shao, Y.M., Miao, S., and Wang, L. (2006). The diversity of the DnaJ/Hsp40 family, the crucial partners for Hsp70 chaperones. Cell. Mol. Life Sci. **63:** 2560–2570.

Rajan, V.B., and D'Silva, P. (2009). Arabidopsis thaliana J-class heat shock proteins: Cellular stress sensors. Funct. Integr. Genomics **9:** 433–446.

Riechmann, J.L., and Meyerowitz, E.M. (1997). MADS domain proteins in plant development. Biol. Chem. **378:** 1079–1101.

Samach, A., Onouchi, H., Gold, S.E., Ditta, G.S., Schwarz-Sommer, Z., Yanofsky, M.F., and Coupland, G. (2000). Distinct roles of CONSTANS target genes in reproductive development of Arabidopsis. Science **288:** 1613–1616.

Schwab, R., Ossowski, S., Riester, M., Warthmann, N., and Weigel, D. (2006). Highly specific gene silencing by artificial microRNAs in *Arabidopsis*. Plant Cell **18:** 1121–1133.

Scidmore, M.A., Okamura, H.H., and Rose, M.D. (1993). Genetic interactions between KAR2 and SEC63, encoding eukaryotic homologues of DnaK and DnaJ in the endoplasmic reticulum. Mol. Biol. Cell **4:** 1145–1159.

Searle, I., He, Y., Turck, F., Vincent, C., Fornara, F., Kröber, S., Amasino, R.A., and Coupland, G. (2006). The transcription factor FLC confers a flowering response to vernalization by repressing meristem competence and systemic signaling in Arabidopsis. Genes Dev. **20:** 898–912.

Sheldon, C.C., Burn, J.E., Perez, P.P., Metzger, J., Edwards, J.A., Peacock, W.J., and Dennis, E.S. (1999). The FLF MADS box gene: A repressor of flowering in *Arabidopsis* regulated by vernalization and methylation. Plant Cell **11:** 445–458.

Silver, P.A., and Way, J.C. (1993). Eukaryotic DnaJ homologs and the specificity of Hsp70 activity. Cell **74:** 5–6.

Simpson, G.G., and Dean, C. (2002). Arabidopsis, the Rosetta stone of flowering time? Science **296:** 285–289.

Sparkes, I.A., Runions, J., Kearns, A., and Hawes, C. (2006). Rapid, transient expression of fluorescent fusion proteins in tobacco plants and generation of stably transformed plants. Nat. Protoc. **1:** 2019–2025.

Takada, S., and Goto, K. (2003). Terminal flower2, an *Arabidopsis* homolog of heterochromatin protein1, counteracts the activation of flowering locus T by constans in the vascular tissues of leaves to regulate flowering time. Plant Cell **15:** 2856–2865.

Tamura, K., Takahashi, H., Kunieda, T., Fuji, K., Shimada, T., and Hara-Nishimura, I. (2007). *Arabidopsis* KAM2/GRV2 is required for proper endosome formation and functions in vacuolar sorting and determination of the embryo growth axis. Plant Cell **19:** 320–332.

Theissen, G. (2000). Plant biology. Shattering developments. Nature **404:** 711–713, 713.

Wang, C.C., and Tsou, C.L. (1998). Enzymes as chaperones and chaperones as enzymes. FEBS Lett. **425:** 382–384.

Wang, W., Vinocur, B., Shoseyov, O., and Altman, A. (2004). Role of plant heat-shock proteins and molecular chaperones in the abiotic stress response. Trends Plant Sci. **9:** 244–252.

Wang, Y., Liu, C., Yang, D., Yu, H., and Liou, Y.C. (2010). Pin1At encoding a peptidyl-prolyl cis/trans isomerase regulates flowering time in Arabidopsis. Mol. Cell **37:** 112–122.

Yang, Y., Qin, Y., Xie, C., Zhao, F., Zhao, J., Liu, D., Chen, S., Fuglsang, A.T., Palmgren, M.G., Schumaker, K.S., Deng, X.W., and Guo, Y. (2010). The *Arabidopsis* chaperone J3 regulates the plasma membrane H^+-ATPase through interaction with the PKS5 kinase. Plant Cell **22:** 1313–1332.

Yu, H., Ito, T., Wellmer, F., and Meyerowitz, E.M. (2004). Repression of AGAMOUS-LIKE 24 is a crucial step in promoting flower development. Nat. Genet. **36:** 157–161.

Yu, H., Xu, Y., Tan, E.L., and Kumar, P.P. (2002). AGAMOUS-LIKE 24, a dosage-dependent mediator of the flowering signals. Proc. Natl. Acad. Sci. USA **99:** 16336–16341.

Yu, H., Yang, S.H., and Goh, C.J. (2000). DOH1, a class 1 knox gene, is required for maintenance of the basic plant architecture and floral transition in orchid. Plant Cell **12:** 2143–2160.

Zhou, R.G., and Miernyk, J.A. (1999). Cloning and analysis of AtJ3 gene in *Arabidopsis thaliana*. Acta Bot. Sin. **41:** 597–602.

Zuo, J., Niu, Q.W., and Chua, N.H. (2000). Technical advance: An estrogen receptor-based transactivator XVE mediates highly inducible gene expression in transgenic plants. Plant J. **24:** 265–273.